THERMO-MECHANICAL DESIGN OF THE EXPERT NOSE AND TESTING OF THE LOAD INTRODUCTIONS

Kornelia Stubicar[(1)], Thomas Reimer[(1)],

[(1)]DLR, Institute of Structures and Design, Pfaffenwaldring 38-40, D-70569 Stuttgart, Germany,
Email:Kornelia.Stubicar@dlr.de , Thomas.Reimer@dlr.de

ABSTRACT

EXPERT is a mission to gather precise in-flight data of the re-entry aerothermodynamic environment [1]. That led to the selection of a ceramic matrix composite heat shield as the Thermal Protection System (TPS) for the nose of the vehicle. The Instrumented Nose Assembly (NAP) is a sub-system of the EXPERT vehicle, consisting of the ceramic matrix composite (CMC) nose and embedded payloads to measure temperature, heat flux and spectroscopic data.
Since EXPERT is a vehicle with a high ballistic coefficient the aerodynamic pressure in the stagnation area reaches a value of 1.5 bar. During re-entry the peak heat flux will reach up to 1.8 MW/m² and the predicted temperatures will reach up to 2050°C in the capsule front.
Due to the very large temperature gradients between hot surface and internal cold structures the problem of mismatching thermal expansion has to be solved. At the same time the nose has to withstand the high pressure loads.
The paper describes the design of the nose and the load introductions attaching the nose to the vehicle. The thermo-mechanical analyses as well as mechanical tests of the load introduction are presented.

INTRODUCTION

Ceramic matrix composites (CMC) are suitable materials for hot structures and thermal protection systems because of their outstanding properties. The nose of the EXPERT vehicle is made from C/C-SiC, a type of CMC developed by DLR Stuttgart. All components made out of this material had to be tested in adequate conditions to qualify them for flight.
The load introduction of the nose assembly is a crucial item for the system. There are hat profiles on the inside of the nose shell that are used to attach metallic components to the nose. The profiles are used to transfer the mechanical loads from the nose into the cold structure of the vehicle (the colander). They are therefore essential components and their proper function has to be verified. In addition to the vibration tests of the complete nose assembly this was done via dedicated mechanical subsystem tests.
A hydraulic test machine was used to create the required test environment for the load introduction tests. These tests were performed only at room temperature conditions.

MISSION OVERVIEW

The EXPERT vehicle will be launched on a Russian Volna rocket on a sub-orbital trajectory. The peak velocity will be 5 km/s, the peak altitude 120 km. Since EXPERT is a vehicle with a high ballistic coefficient of roughly 1000 kg/m² the aerodynamic pressure in the stagnation area reaches a value of 1.5 bar. During re-entry the peak heat flux will reach up to 1.8 MW/m² and the predicted temperatures will reach up to 2050°C in the capsule front.
The launch will be in 2010.

NOSE DESIGN

There are large temperature gradients between the hot nose and the internal cold structure. In the stagnation area 2050°C are expected whereas the substructure remains practically at room temperature with a distance of 50 mm between them. Therefore, the problem of mismatching thermal expansion has to be solved.
At the same time the nose has to withstand high vibration and shock loads during launch and high pressure loads during re-entry. So the essential requirements from a mechanical standpoint are stiffness, a high load capability in general and the capability to compensate for the thermal expansion mismatch.
A kinematic solution for the expansion mismatch was investigated briefly but not followed for a long time. Instead, a design that relies on the elastic deformation of certain components was preferred. Fig. 1 shows the nose with assembled load introduction components and Fig. 2 shows the individual load introduction parts. An important issue was that

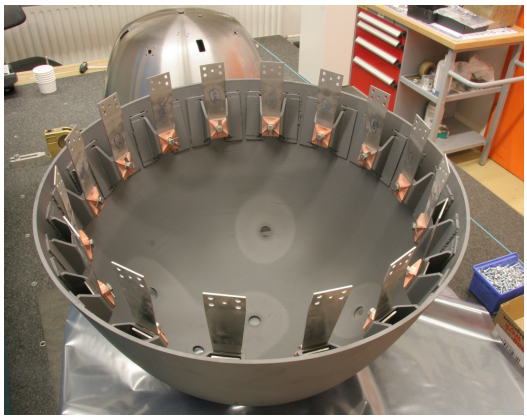

Fig. 1: CMC nose with load introductions

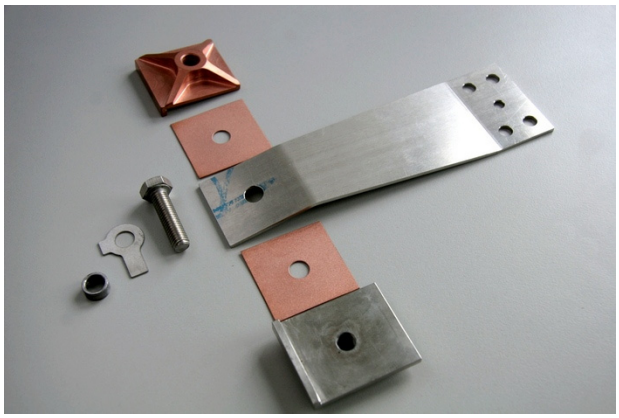

Fig. 2: Load introduction components

metallic fasteners should be used which necessitates a location for the fastener in a low temperature region. That consideration resulted in the introduction of the profiles on the inside of the nose.
The advantages of the design are that it is simple, easy to install and uses a metallic fastener. In addition there are no disturbances on the nose surface due to bolt heads which might create problems with regard to laminar to turbulent transition of the flow.

NUMERICAL ANALYSIS

The temperature at the metallic fastener is always low during the mission. Only after landing it rises to roughly 350°C. The nose assembly was analysed via FEM. It became clear soon that the most crucial components are the hat profiles in the nose with regard to mechanical stress. The calculations were done as thermo-mechanical analyses including thermal loads and pressure loads in the re-entry case. For the launch cases, random vibration analysis was done as well as quasi-static analyses that reflect the random vibration loads.
The thermo-mechanical calculations of the re-entry case showed low stresses over the nose in general at below +30MPa as shown in Fig. 4. Also in the hat profiles the stress is below +30MPa depicted in Fig. 3. The material allowables for C/C-SiC are +80MPa in tension and +120 MPa in bending and -200 MPa in compression.
A detailed investigation of the bond between the hat profile and the nose shell was carried out to verify the bond strength. The goal was to minimise the stress in the bond to very low levels.

The random vibration loads were analysed directly with a random vibration analysis. The calculations showed that the metallic bracket is in fact the most critical component. After the random vibration analysis with the complete model of the nose assembly, a static analysis was carried out with a submodel of one of the load introductions shown in Fig. 5. The input for the submodel analysis was the displacement result of the random vibration analysis of the complete nose assembly. The submodel included more detailed and realistic contact conditions than the complete model. The highest stresses could be observed around the bolt holes with a peak level of 200 MPa shown in Fig. 6.

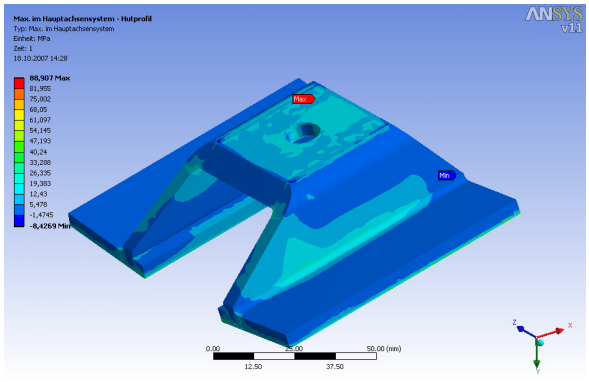

Fig. 3: Stress in the hat profile

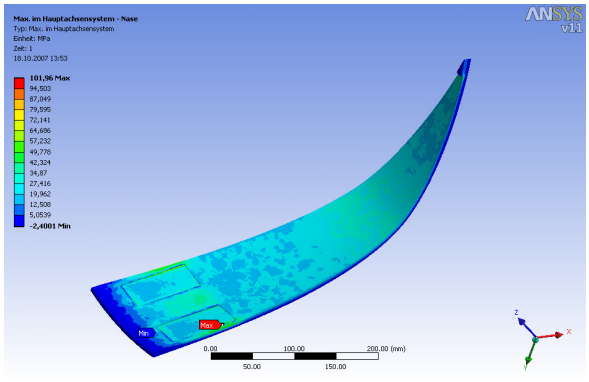

Fig. 4: Stress in the nose shell

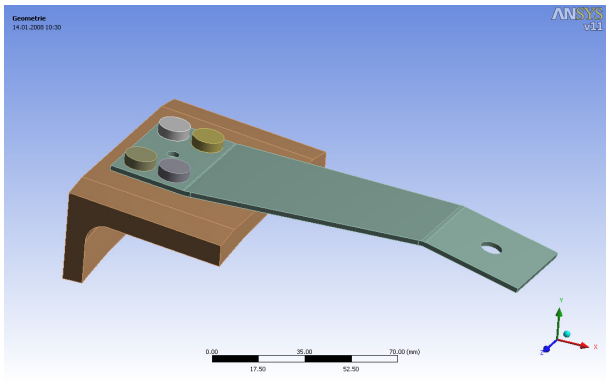

Fig. 5: Submodel of the metallic load introduction

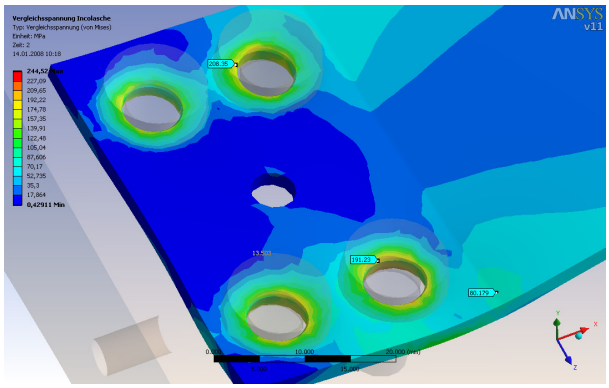

Fig. 6: Stress in the metallic bracket

This is not critical in terms of the static material allowable. However, when it is considered that the launch is a dynamic environment the stress has to be evaluated with regard to that. This means that the lifetime of the component has to be determined under that load. The problem is that there is only very little fatigue data available and there was not enough time to generate the relevant fatigue data before the qualification tests. So an effort was made to estimate the bracket lifetime with the data available and assess the situation. It was found that it is very difficult to arrive at a reliable lifetime prediction since small uncertainties in some parameters used in the lifetime determination have a big impact on the results. The lifetime determination was based on a methodology developed for the use with electronic printed circuit boards (PCB), described by Steinberg [2]. The lifetime of the metallic bracket was found to be long enough to withstand the vibration loads, however, with only a small margin. Ultimately, the vibration tests that were carried out later showed, that all components were well designed.

A buckling analysis was carried out with the load introduction components. The buckling load was determined to be 24.8 kN which results in a margin of safety of 5.5 against buckling of the bracket. So buckling is uncritical.

LOAD INTRODUCTION TEST SET-UP

The load introduction test samples were made from the same material as the nose. The test was set up as an axial compression test.

A Zwick 1484 was used as test facility. It is a universal axial testing machine often used for standard tests to investigate material parameters.

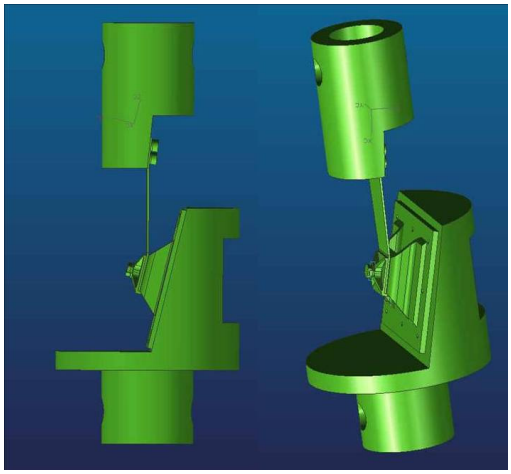

Fig. 7: Attachment fittings for the test

The function of the ceramic nose is to keep the aerodynamic contour during re-entry and withstand the pressure load. The resulting loads have to be introduced into the attachment fittings. Therefore two fixtures were manufactured. One part has a cavity where the nose sample can be put in and fixed. The other part represents the colander. Fig. 7 shows the CAD model of the attachment fixtures for the Zwick facility:

These two attachment fixtures with the mounted test components were fixed on the machine as shown in Fig. 8. During test the components get compressed till the compression load leads to a failure in the test component. The target was to reach a minimum load of 3,75 kN before a structural failure appears. Two cameras were used in addition to the data acquisition, also visible in Fig. 8. Each sample was checked in the Computer tomograph before testing.

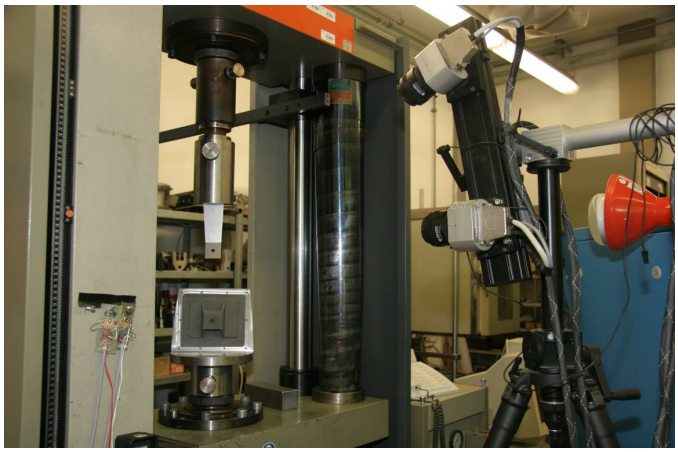

Fig. 8: Fixture with sample parts

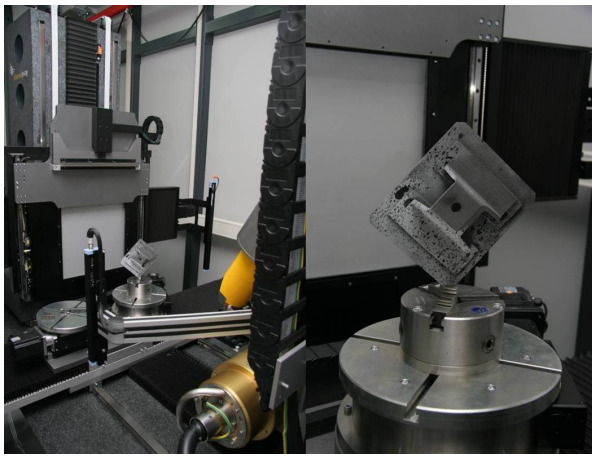

Fig. 9: Computer tomography

Table 1: Test variables

	Amount:	Hat profil:	Material:	Plate:	Reinforcement:	Temp.:
a	6	0°/90°	XB	45°	yes	cold
b	6	45°	XB	45°	no	cold
c	6	45°	XB	45°	yes	cold
d	6	45°	XB-T800	45°	yes	cold
e	6	0°/90°	XB	0°/90°	yes	cold
f	2	45°	XB	0°/90°	yes	cold
	∑ 32					

Test variable

The test articles were divided into 6 groups (a-f). Each group is characterised by a specific test variable, e.g. the lay-up of the hat profiles from group (a) is made with a 0°/90° fibre orientation whereas the lay-up of group (b) is done with +/- 45°; see Table 1.
The reinforcement is an extra CMC component surrounding the hat profile foot to minimise stress concentrations at the interface between hat profile and plate (nose), see Fig. 13.

In total there were 32 components to be tested. Group (d) is the one that represents the lay-up of the nose hardware for EXPERT.

TEST RESULTS

The results of the 32 test samples are shown below. During testing two failure modes were observable. One is characterised by failure of the bond interface between the profile and the plate shown in Fig. 12. In the other failure mode, the profile cracks in the profile top section, illustrated in Fig. 13.

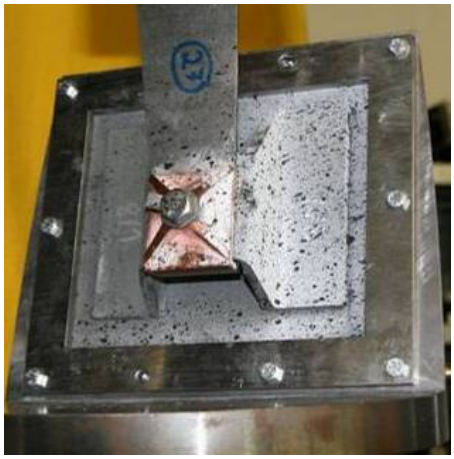

Fig. 10: Sample before testing

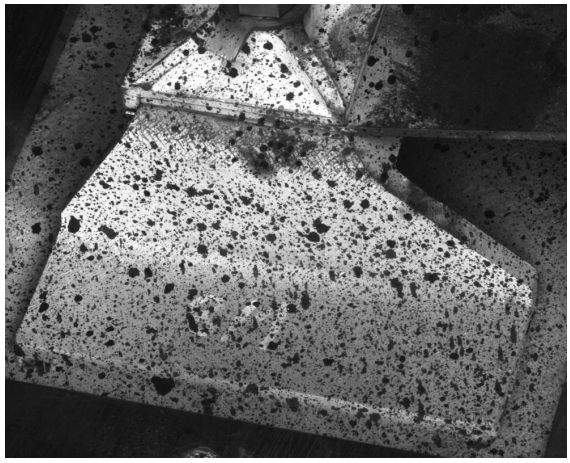

Fig. 11: Sample before test – camera view

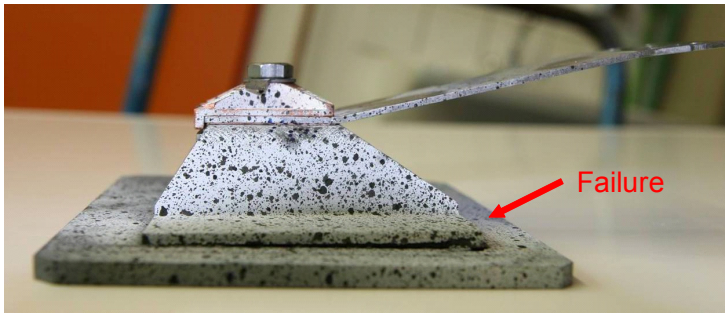

Fig. 12: Sample after test – bonding failure

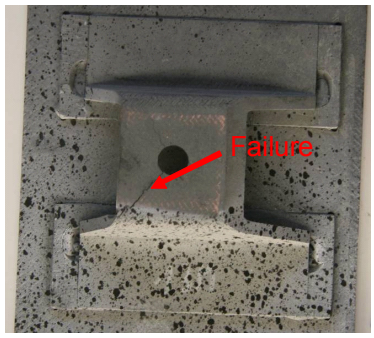

Fig. 13: Sample after test – crack failure in profile top

The recorded compression loads over the deflection and the maximum compression load at failure on each hat profile lead to the following results: The average value for the maximum compression load for all 32 test articles is 12,28 kN. All qualification tests were performed successfully. The specification load to be reached for each hat profile was 3,75 kN and was exceeded on an average three times.
The cracking failure in the hat profile top or the failure in the bonding happened to appear at a ratio of almost 1:1. Also the averages of the maximum compression load for both types of failure are similar as shown in Fig. 14.
No significant differences could be found, which caused the types of failure. The hat profiles with the fibre orientation 0°/90° seemed to have an affinity to crack in hat profile top. The direction of the crack in hat profile top was always in direction of the hat profile fibre orientation.

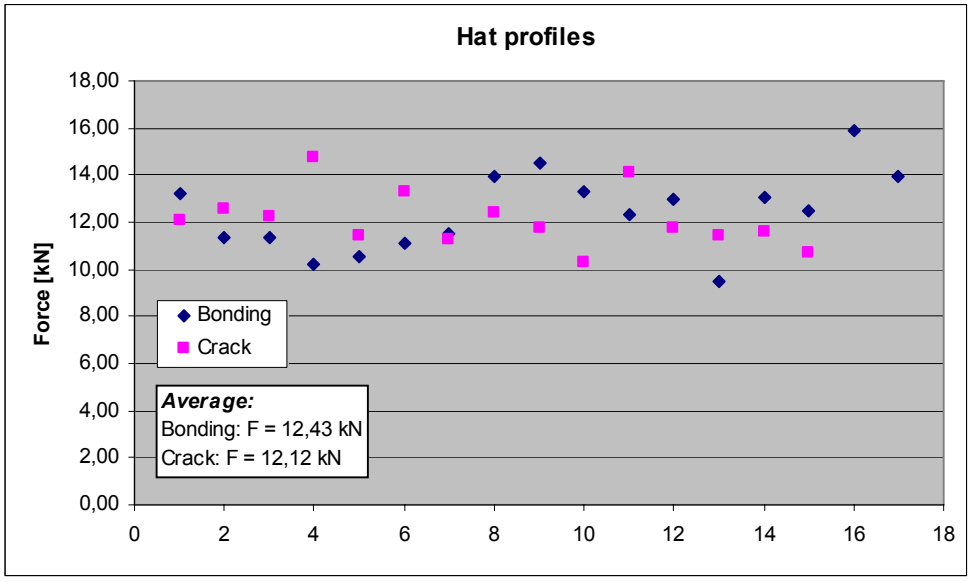

Fig. 14: Comparison of failure types

In Table 2 the test data is displayed with the testing variables. From that the following statements can be made: Comparing the fibre orientation 0°/90° and ±45° of the hat profiles attached on plates with a fiber orientation of ±45° (purple testing variable)as shown in Fig. 15 there are no significant differences. The fibre orientation of the hat profiles of ±45° can sustain slightly higher loads on average than the fibre orientation of 0°/90°.

Table 2: Displayed test variables from table 2

Test Variable	#	Hat Profile	Clip	Reinforcing	Failure [kN]	Failure	Tightening Torque[Nm]	Sand Blasted	Material	Type of Fiber	Fiber Orientation Hat profile	Fiber Orientation Plate
a	19	**31/1**	30	yes	**9,50**	Bonding	17	yes	XB	HTA	0° / 90°	±45° / ±45°
a	20	**31/2**	30	yes	**11,28**	Crack	17	yes	XB	HTA	0° / 90°	±45° / ±45°
a	21	**30/1**	30	yes	**12,41**	Crack	17	yes	XB	HTA	0° / 90°	±45° / ±45°
a	22	**30/2**	29	yes	**11,77**	Crack	17	yes	XB	HTA	0° / 90°	±45° / ±45°
a	23	**32/1**	29	yes	**13,08**	Bonding	17	yes	XB	HTA	0° / 90°	±45° / ±45°
a	24	**32/2**	29	yes	**12,49**	Bonding	17	yes	XB	HTA	0° / 90°	±45° / ±45°
b	1	**9/1**	30	no	**12,11**	Crack	12	no	XB	HTA	±45° / ±45°	±45° / ±45°
b	4	**8/2**	27	no	**11,32**	Bonding	12	no	XB	HTA	±45° / ±45°	±45° / ±45°
b	5	**9/2**	29	no	**10,23**	Bonding	12	yes	XB	HTA	±45° / ±45°	±45° / ±45°
b	10	**8/1**	27	no	**11,52**	Bonding	17	yes	XB	HTA	±45° / ±45°	±45° / ±45°
b	11	**11/1**	27	no	**13,97**	Bonding	17	yes	XB	HTA	±45° / ±45°	±45° / ±45°
b	16	**11/2**	30	no	**13,26**	Bonding	17	yes	XB	HTA	±45° / ±45°	±45° / ±45°
c	2	**10/1**	28	yes	**13,18**	Bonding	12	no	XB	HTA	±45° / ±45°	±45° / ±45°
c	3	**10/2**	29	yes	**11,38**	Bonding	12	no	XB	HTA	±45° / ±45°	±45° / ±45°
c	12	**13/2**	30	yes	**14,55**	Bonding	17	yes	XB	HTA	±45° / ±45°	±45° / ±45°
c	13	**13/1**	30	yes	**14,79**	Crack	17	yes	XB	HTA	±45° / ±45°	±45° / ±45°
c	14	**14/2**	29	yes	**11,46**	Crack	17	yes	XB	HTA	±45° / ±45°	±45° / ±45°
c	15	**14/1**	29	yes	**13,30**	Crack	17	yes	XB	HTA	±45° / ±45°	±45° / ±45°
d	6	**23/2**	30	yes	**10,53**	Bonding	15	yes	XB-T800	T800	±45° / ±45°	±45° / ±45°
d	7	**24/2**	30	yes	**12,56**	Crack	17	yes	XB-T800	T800	±45° / ±45°	±45° / ±45°
d	8	**23/1**	29	yes	**11,07**	Bonding	17	yes	XB-T800	T800	±45° / ±45°	±45° / ±45°
d	9	**25/2**	29	yes	**12,27**	Crack	17	yes	XB-T800	T800	±45° / ±45°	±45° / ±45°
d	17	**25/1**	30	yes	**12,33**	Bonding	17	yes	XB-T800	T800	±45° / ±45°	±45° / ±45°
d	18	**24/1**	30	yes	**13,01**	Bonding	17	yes	XB-T800	T800	±45° / ±45°	±45° / ±45°
e	27	**34/1**	29	yes	**10,29**	Crack	17	yes	XB	HTA	0° / 90°	0° / 90°
e	28	**34/2**	30	yes	**14,11**	Crack	17	yes	XB	HTA	0° / 90°	0° / 90°
e	29	**35/2**	30	yes	**11,76**	Crack	17	yes	XB	HTA	0° / 90°	0° / 90°
e	30	**36/1**	29	yes	**11,43**	Crack	17	yes	XB	HTA	0° / 90°	0° / 90°
e	31	**36/2**	30	yes	**11,57**	Crack	17	yes	XB	HTA	0° / 90°	0° / 90°
e	32	**38/2**	30	yes	**10,67**	Crack	17	yes	XB	HTA	0° / 90°	0° / 90°
f	25	**33/1**	29	yes	**15,89**	Bonding	17	yes	XB	HTA	±45° / ±45°	0° / 90°
f	26	**33/2**	29	yes	**13,98**	Bonding	17	yes	XB	HTA	±45° / ±45°	0° / 90°

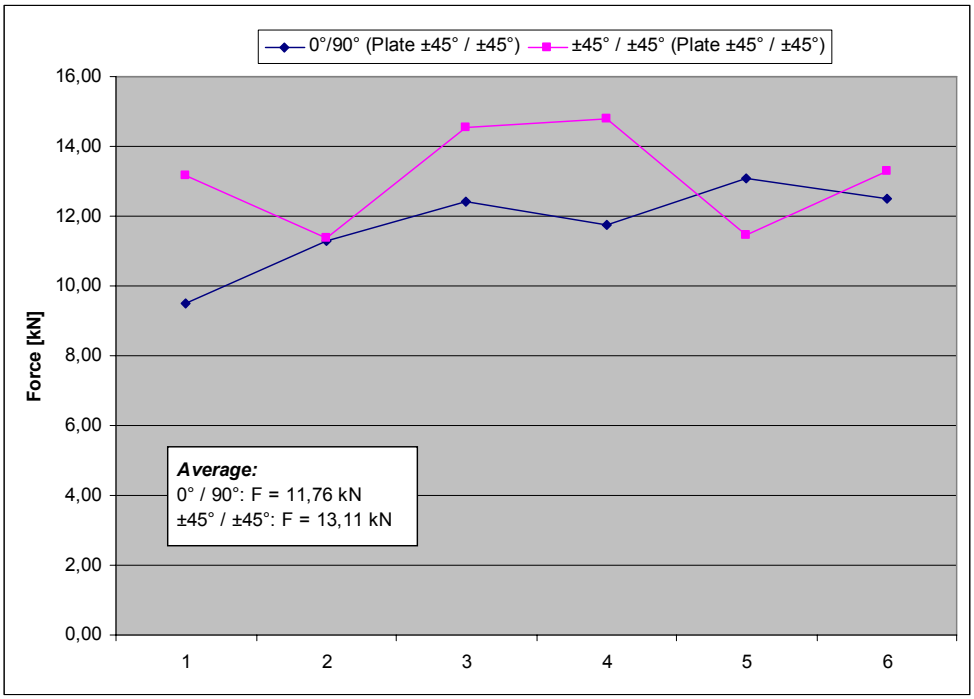

Fig. 15: Influence of the fibre orientation in the hat profile on the load introduction strength using a ±45° plate.(purple testing variable)

The Comparison of hat profiles with and without a reinforcement with both the profiles and the plates having ±45° fibre orientation (blue testing variable) shows that with a reinforcement the system can take on average 8.6 % higher loads than a without see Fig. 16.

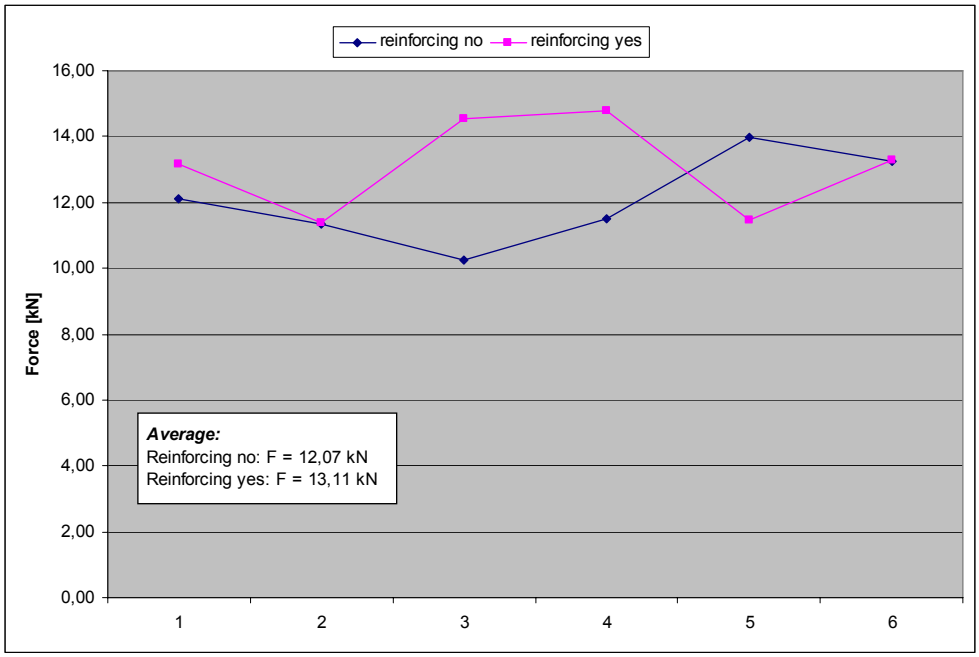

Fig. 16: Influence of the reinforcement at the hat profile on the load introduction strength using ±45° profiles and plates (blue testing variable)

Another testing variable was the fibre type. Either HTA or T800 fibres were used (green testing variable) described as XB material (HTA fibre) and XB-T800. The comparison in Fig. 17shows, that both fibres are suitable, but that the use of the HTA fibres results on average in a 9.6% higher strength.

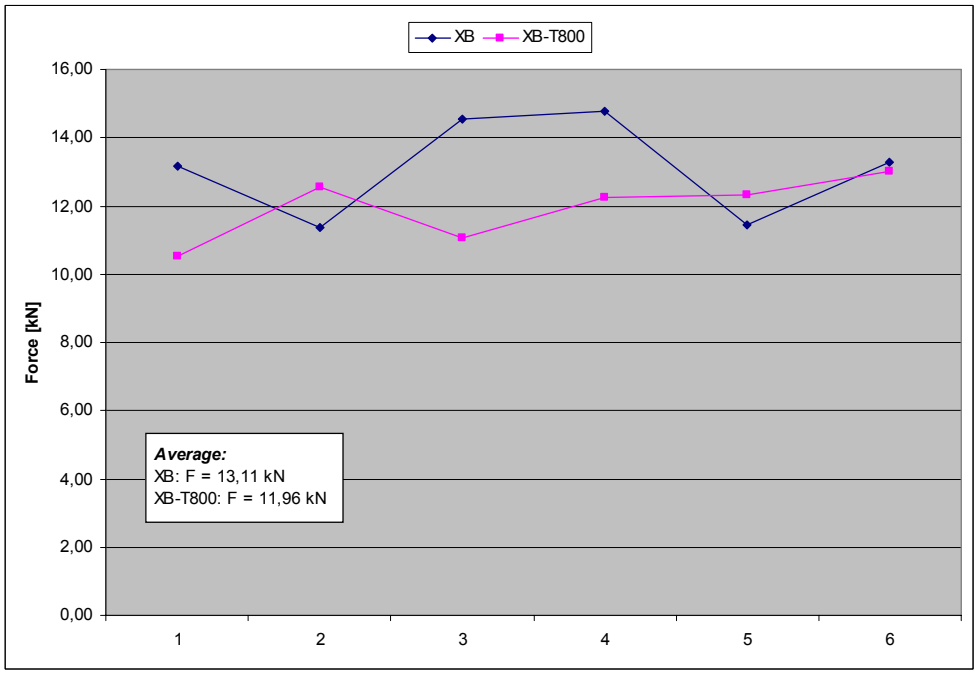

Fig. 17: Influence of the fibre type in the hat profile on the load introduction strength using ±45° profiles and plates (green testing variable)

Comparing the fibre orientation 0°/90° and ±45° of the hat profiles bonded on plates with a fiber orientation of 0°/90° shown in Fig. 18 (yellow testing variable), there is a significant difference. The fibre orientation of the hat profiles of ±45° apparently sustains 28% higher loads on average than the fibre orientation of 0°/90°. However, it has to be noted that there were only 2 tests performed with that configuration.

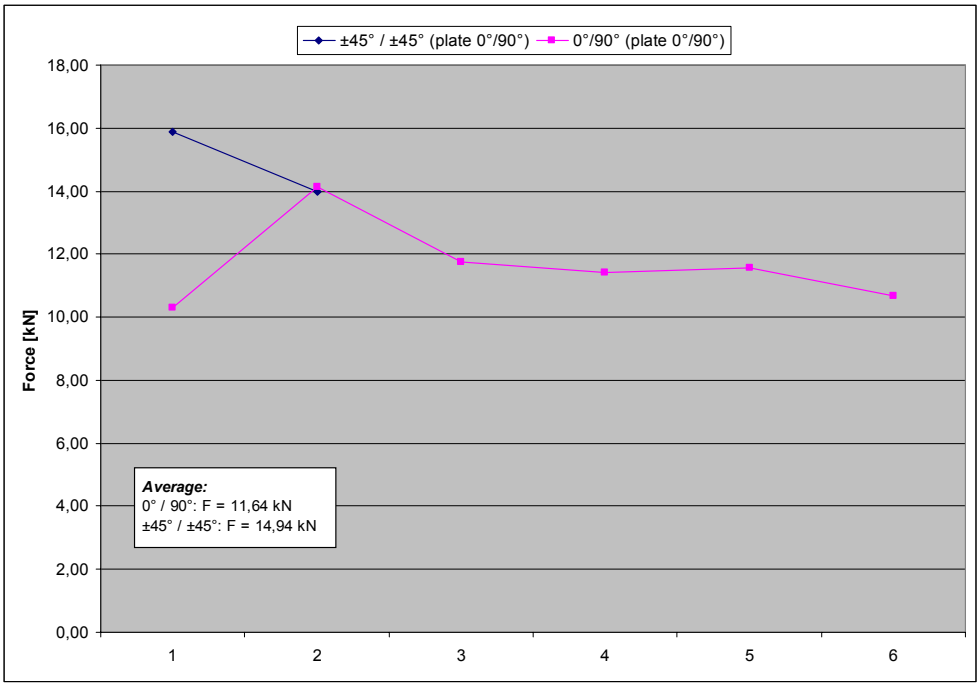

Fig. 18: Influence of the fibre orientation in the hat profile on the load introduction strength using 0°/90° plates (yellow testing variable)

CONCLUSION

The numerical analysis of the nose of EXPERT showed that the critical components in the design are the load introductions that attach the nose to the metallic cold structure. Therefore, mechanical tests were conceived and set up to verify the strength of the components.
Since the analysis also showed that the temperature of the relevant components is low at the time of the highest mechanical loads it was decided to carry out the tests at room temperature to limit the required test effort.
The tests were carried out on samples that represent one single load introduction out of 16 in the nose. The geometry of the samples was adapted slightly from the curved shape of the nose into a flat plate with the hat profile bonded onto the plate. The load was applied as an axial compression load.
Two failure modes could be observed. The samples failed either due to bond failure between profile and plate or due to cracking of the profile top with both failure types at roughly the same load. The failure load was on average 12.28 kN over all samples which results in a margin of safety of 2.27.
When different test parameters are evaluated there is a homogeneous picture. All the variations performed more or less equally well and none of the investigated parameters is critical with regard to the load introduction performance.
With that result it can be concluded that the selected design is suitable to be used in the flight model of the nose for the EXPERT vehicle.

REFERENCES

[1] Gavira, J., “EXPERT - A European Aerothermodynamics In-Flight Testbed”, Proceedings 6th European Workshop on Thermal Protection Systems and Hot Structures, 1-3 April 2009, Stuttgart, Germany
[2] Steinberg, D.S., ”Vibration Analysis for Electronic Equipment”, 3rd Ed., Wiley & Sons, New York, 2000